Vietnam Journal of Catalysis and Adsorption
Tạp chí xúc tác và hấp phụ Việt Nam

https://jca.edu.vn

Development and Characterization of Antimicrobial PLA/PVA/Ag Nanocomposite Films for Food Packaging Applications

Nguyen Ngoc Son[1], Vu Quang Hung[1], Ly Quoc Vuong[1], Doan Tuan Anh[1], Vu Minh Thanh[1]
Vu Thanh Dong[2] , Nguyen Thi Huong[1,*]

[1] *Institute of Materials, Biology and Environment, 17 Hoang Sam Street, Hanoi, Vietnam.*
[2] *Department of Materials Science and Engineering, Kangwon National University, Samcheok 25912, Republic of Korea*
** Email: nguyenhuong0916@gmail.com*

ARTICLE INFO

Received: 29/07/2025
Accepted: 25/08/2025
Published: 30/09/2025

Keywords:
Antimicrobial film;
Polylactic acid (PLA);
Silver nanoparticles (AgNPs);
Food packaging;
Polyvinyl alcohol (PVA)

ABSTRACT

This study presents the fabrication and characterization of biodegradable nanocomposite films based on a Polylactic acid (PLA) matrix, incorporating Polyvinyl alcohol (PVA) and silver nanoparticles (AgNPs), for active food packaging applications. PVA/Ag nanocomposites were synthesized via an ultrasound-assisted chemical reduction method before their integration into the PLA matrix using a solvent casting technique. Characterization analyses (FT-IR, SEM, TEM) confirmed the successful formation of the composite material with a relatively uniform dispersion of silver nanoparticles within the polymer matrix. The PLA/PVA/Ag film with a 1.0 wt% content (F/1.0) exhibited optimal mechanical properties, with a tensile strength of 5.77 MPa, nearly 20% higher than the neat PLA control film. Notably, the composite material demonstrated broad-spectrum antimicrobial activity, effectively inhibiting the growth of *B. subtilis*, *E. coli*, and *S. cerevisiae* in a dose-dependent manner. These findings affirm the potential of PLA/PVA/Ag films as an advanced, sustainable, and effective packaging material for the food preservation industry.

Introduction

The global plastic pollution crisis has prompted a significant shift in the packaging industry towards sustainable and biodegradable materials [1,2]. Among various biopolymers, Polylactic acid (PLA) has emerged as one of the most viable alternatives to petroleum-based plastics, owing to its renewable origins, microbial degradability, and approval by the U.S. Food and Drug Administration (FDA) for direct food contact applications. PLA films can be industrially produced at a relatively low cost through common standard techniques such as solvent casting and extrusion [3].

However, applying PLA as an active packaging material faces two inherent limitations. Firstly, neat PLA exhibits low toughness, with an elongation at break of only 1–12% [4,5], rendering the material brittle and susceptible to mechanical failure. Furthermore, PLA is biologically inert, completely lacking the natural antimicrobial activity required to combat food spoilage microorganisms [6,7]. Therefore, simultaneously improving both the mechanical properties and antimicrobial capabilities is an urgent requirement to enhance the value of PLA films [6,8].

AgNPs have been demonstrated to be a highly effective antimicrobial agent for PLA matrices. The mechanism of

https://doi.org/10.62239/jca.2025.037
50

action for AgNPs is based on the release of Ag^+ ions through oxidative dissolution [9], which interact with sulfur-containing, amine, and phosphate functional groups in microbial cells [9,10]. Concurrently, they generate free radicals, inducing oxidative stress. For instance, Ghazvini et al. (2023) demonstrated that PLA/AgNPs films could completely eradicate E. coli bacteria after 120 minutes of contact [11]. Notably, AgNPs with a size of 10-15 nm exhibit optimal stability, biocompatibility, and antimicrobial activity [9].

A recent study (2020) successfully developed PLA/AgNPs nanocomposite fibers via an in-situ reduction method, achieving a 94.86% reduction of E. coli and 74.91% of S. aureus after 120 minutes [12]. Furthermore, AgNPs have also been reported to potentially improve the mechanical properties of PLA when well-dispersed. For instance, one study showed a 20% increase in tensile strength upon the addition of AgNPs, while the material remained compliant with food safety standards with low silver migration levels [13]. Studies show that antimicrobial efficacy depends on the active agent's concentration, nanoparticle size, and dispersion method within the PLA matrix, opening prospects for developing intelligent active packaging systems with AgNPs playing a key role in the food industry. However, a major challenge is that the dispersion of silver nanoparticles in the hydrophobic PLA matrix is often non-uniform, leading to agglomeration that reduces antimicrobial efficacy and negatively affects mechanical properties [14,15].

This is where Polyvinyl alcohol (PVA) plays a pivotal role. With its biocompatible nature and abundance of hydroxyl groups [16,17], PVA not only improves the ductility of PLA films [18] but also acts as an ideal stabilizer and carrier for silver nanoparticles [19]. Synthesizing silver nanoparticles directly in a PVA solution (the ex-situ method) helps prevent agglomeration and ensures a uniform dispersion of the nanoparticles in the final PLA film [20].

A favorable interaction among the three components PLA, PVA, and AgNPs is expected to create a composite material with superior properties. Therefore, this study was conducted to systematically fabricate and evaluate PLA/PVA/Ag nanocomposite films. Specifically, the research focuses on: (i) synthesizing a stable PVA/Ag nanocomposite via an ultrasound-assisted chemical reduction method; (ii) fabricating PLA/PVA/Ag films with varying nanocomposite contents; and (iii) investigating the influence of the nanocomposite content on the mechanical, physicochemical, and especially the antimicrobial properties, thereby identifying an optimal formulation for potential applications.

Experimental

Chemical

Polylactic acid (PLA, Mw = 260,000 g/mol) and polyvinyl alcohol (PVA, Mw = 9,000–10,000 g/mol) were of commercial grade and obtained from a supplier in the USA. Silver nitrate ($AgNO_3$) and glucose were purchased from Merck (Germany). Solvents, including dichloromethane (DCM) and absolute ethanol, were of analytical grade and supplied by Fisher BioReagents™. Ammonia solution (25%, Emsure) adjusted the pH during synthesis. All chemicals were used as received without further purification.

Methods

Synthesis of PVA/Ag Nanocomposite

The PVA/Ag nanocomposite was synthesized based on an ultrasound-assisted chemical reduction of Ag^+ ions to metallic silver (Ag^0). In this process, PVA was a stabilizing and capping agent, while glucose acted as the reducing agent.

Specifically, 50 mL of a 100 ppm $AgNO_3$ solution was added dropwise at a rate of 5 mL/min to a 500 ppm PVA solution under continuous magnetic stirring. Throughout this process, a 25% ammonia (NH_3) solution was added to adjust and maintain the mixture's pH in the range of 9–10. The reaction mixture was then sonicated using a VCX130 probe sonicator operating at a frequency of 40 kHz for 10 minutes. Subsequently, 5 mL of a 1M glucose solution was added to the system, and sonication was continued for 30 minutes to ensure the complete reduction of silver ions. The formation of silver nanoparticles was visually observed through the color change of the solution from colorless to pale yellow, and finally to a characteristic dark yellowish-brown. The resulting PVA/Ag colloidal solution was stored in a dark glass bottle to prevent photodegradation before further use.

Fabrication of PLA/PVA/Ag Nanocomposite Films

The PLA/PVA/Ag nanocomposite films were fabricated using a solvent casting technique. First, solution A was prepared by completely dissolving 1.6 g of PLA in 75 mL of dichloromethane (DCM), assisted by an ultrasonic bath for 30 minutes. Concurrently, suspension B was prepared by dispersing a required amount of the PVA/Ag colloidal solution into 10 mL of ethanol, followed by treatment with a probe sonicator for 10 minutes to ensure homogeneous dispersion.

Next, suspension B was added dropwise into solution A at a rate of 1 mL/min under magnetic stirring. The final

https://doi.org/10.62239/jca.2025.037

mixture was subjected to further probe sonication for 30 minutes to enhance the dispersion of the PVA/Ag phase within the PLA polymer matrix, resulting in solution C.

To cast the film, 50 mL of solution C was poured onto a flat polytetrafluoroethylene (PTFE) substrate (12 cm × 25 cm) and spread evenly using a casting knife. The film was allowed to air-dry at room temperature for 3–4 hours to evaporate the solvent. After being peeled from the substrate, the film was placed in a vacuum oven at 30 °C for 12 hours to completely remove any residual solvent.

The final product was a transparent thin film. This procedure was repeated to fabricate film samples with different PVA/Ag nanocomposite contents: 0.5%, 1.0%, and 1.5% (by weight relative to PLA). These percentages were calculated based on the mass of the solid content (PVA and Ag) in the nanocomposite colloid relative to the initial mass of PLA (1.6 g). The finished films were stored in sealed bags to protect them from moisture and direct light.

Characterization and Evaluation Methods

Structural and Morphological Analysis

Fourier-Transform Infrared Spectroscopy (FT-IR): The chemical structure and interactions between components in the nanocomposite film were analyzed by identifying characteristic functional groups. Spectra were recorded on an FT-IR instrument in the wavenumber range of 4000 to 400 cm^{-1}. Scanning Electron Microscopy (SEM) and Energy-Dispersive X-ray Spectroscopy (EDX): The surface morphology, cross-section, and dispersion of silver nanoparticles in the polymer matrix were investigated using SEM. The elemental composition of the film was semi-quantitatively determined using an EDX system integrated with the SEM instrument.

Evaluation of Mechanical and Physical Properties

Thickness Measurement: The film thickness was measured using a digital micrometer (Mitutoyo, Model PCM 137, No.2046S, Japan). Measurements were taken at five random positions on each sample (four corners and the center), and the average value was reported.

Water Solubility: Film samples were cut into 3×3 cm squares, dried in a vacuum oven at 60°C to a constant weight to determine the initial dry mass (W_0). The dried samples were then immersed in 20 mL of distilled water and gently agitated for 24 hours at room temperature (25°C). After immersion, the insoluble portion of the film was removed, dried again under the same conditions to determine the final dry mass (Wf). The water solubility (S, %) was calculated using the formula:

$$S\ [\%] = \frac{W_0 - W_f}{W_0} \times 100\% \quad (1)$$

Tensile Strength (TS): Mechanical properties, including tensile strength and elongation at break, were determined according to the ASTM D882 standard using a universal testing machine.

Antimicrobial Activity Assay

The antimicrobial activity of the films was quantitatively evaluated using a direct contact colony counting method against test strains *Bacillus subtilis* ATCC 9/58, *Escherichia coli* ATCC 25922, and *Saccharomyces cerevisiae*. Specifically, UV-sterilized film samples were placed into flasks containing a microbial suspension of a predetermined initial concentration and incubated with shaking at 37°C for 24 hours, alongside a control sample without any film. After incubation, the suspension from each flask was serially diluted, spread-plated onto nutrient agar plates, and incubated for another 24 hours. The antimicrobial efficacy was determined by counting the surviving colony-forming units (CFU/mL) in each sample compared to the control.

Results and discussion

Effect of PVA/Ag Nanocomposite Content on the Mechanical Properties of the Films

The composite films were fabricated using a solvent casting technique. The thickness of the films and their uniformity are critical factors. The results in Table 1 show that the average thickness of the nanocomposite films ranges from 0.064 to 0.069 mm. Although there is slight variation in the mean thickness, an Although there is slight variation in the mean thickness, an Analysis of Variance (ANOVA) confirmed that this difference is not statistically significant ($F(3, 16) = 0.386$, $p = 0.765$). This indicates that the solvent casting process was well-controlled, producing films of relatively uniform thickness, which is an important factor for ensuring consistency in the evaluation of other mechanical properties.

Table 1: Thickness measurement results of PLA/PVA/Ag films

Conc.	1	2	3	4	5	Avg. (mm)	SD
F/0.0	0.069	0.071	0.073	0.066	0.068	0.069	0.0027
F/0.5	0.079	0.076	0.059	0.052	0.054	0.064	0.0123
F/1.0	0.074	0.072	0.063	0.056	0.058	0.064	0.0075
F/1.5	0.052	0.059	0.084	0.077	0.072	0.069	0.0125

https://doi.org/10.62239/jca.2025.037

The mechanical properties of the films, which determine the load-bearing capacity and toughness of the packaging material, are presented in Table 2. The results in Table 2 indicate that the addition of the PVA/Ag nanocomposite to the PLA matrix profoundly affects the mechanical and elastic properties of the material.

Table 2: Mechanical properties of PLA/PVA/Ag films

Samples	Tensile Strength (MPa)	Elongation at Break (%)
F/0.0	4.83	1.33
F/0.5	5.16	0.97
F/1.0	5.77	0.68
F/1.5	3.49	0.57

Compared to the neat PLA control film (F/0.0), which had a tensile strength of 4.83 MPa, the addition of PVA/Ag at low concentrations significantly improved this property. Specifically, the F/1.0 film demonstrated superior tensile strength, reaching 5.77 MPa, nearly 20% higher than the original PLA film. This improvement confirms the role of the PVA/Ag nanocomposite as an effective reinforcing agent. At a 1.0% concentration, the nanoparticles are thought to be uniformly dispersed within the polymer matrix, creating good interfacial interaction,facilitating effective stress transfer and hinders the propagation of micro-cracks. However, when the PVA/Ag content increased to 1.5%, the tensile strength decreased sharply to 3.49 MPa, a value lower than the PLA control. This phenomenon is explained by the agglomeration of nanoparticles at high concentrations [21]. These agglomerates no longer act as reinforcements but instead become stress concentration points, creating defects and weakening the overall structure of the material, leading to premature failure. Although TEM images (Figure 2) show good dispersion of individual nanoparticles, agglomeration at the 1.5% concentration may occur on a larger micro-scale not observed, thereby reducing the reinforcing efficiency.

Elongation at break (%E) is a critical indicator of the material's ductility and deformability. The results show that the elongation at break decreases continuously as the PVA/Ag content increases. This demonstrates that the material becomes stiffer and more brittle. This continuous decrease in elongation indicates an increase in the material's stiffness, which consequently suggests a higher elastic modulus. The addition of the PVA/Ag nanoparticles, which constitute a rigid solid phase, into the PLA polymer matrix restricts the movement and sliding of the polymer chains [22]. This restriction reduces the system's mobility, making the material more resistant to deformation under force, which in turn increases its stiffness and elastic modulus while simultaneously reducing its ductility.

Based on this comprehensive analysis, the F/1.0 film is identified as the optimal formulation. This sample not only exhibits a significant improvement in mechanical strength (nearly 20%) compared to the neat PLA film but also represents the best balance between strength and stiffness. Meanwhile, using a higher concentration (1.5%) results in a detrimental effect, degrading the mechanical properties. Therefore, the F/1.0 film, with its superior properties, is the most suitable choice for subsequent studies on food preservation capabilities.

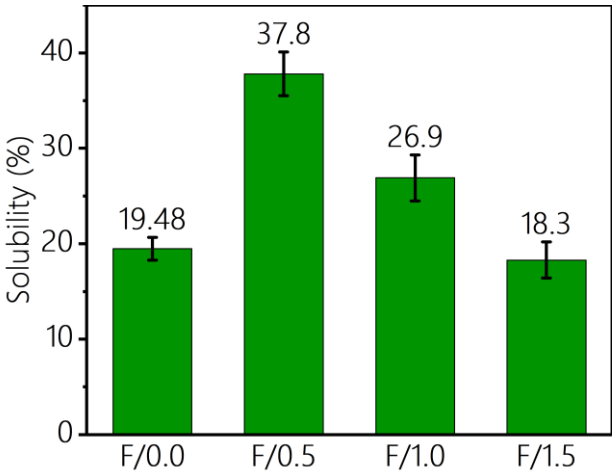

Figure 1: Water solubility of PLA/PVA-Ag films

The experimental results regarding the water solubility of the PLA/PVA-Ag films (Figure 1) reveal a non-linear and significant relationship between the PVA/Ag nanocomposite content and the film's water solubility. Compared to the neat PLA control film (F/0.0), which had a solubility of 19.5%, adding 0.5% PVA/Ag caused a sharp increase in solubility to a peak of 37.8%. This increase is directly attributed to the hydrophilic and water-soluble nature of the PVA component, which is readily leached out from the hydrophobic PLA matrix.

However, a paradoxical trend emerged as the PVA/Ag content was further increased to 1.0% and 1.5%, with the solubility decreasing to 26.9% and 18.3%, respectively. This phenomenon indicates a change in the material's microstructure. At higher concentrations, it is hypothesized that the PVA/Ag nanoparticles act as a reinforcing agent, creating a denser physical interaction network (such as hydrogen bonds) with the PLA chains. This structure becomes more compact, capable of "locking" the PVA molecules in place and hindering water penetration.

The most notable point is that the F/1.5 film (18.3%) exhibited better water resistance than the original neat

https://doi.org/10.62239/jca.2025.037

PLA film (19.5%). This strongly supports the hypothesis of structural improvement. The dispersed nanoparticles in the polymer matrix create a barrier effect, forming a tortuous path that slows the diffusion of water molecules. Therefore, it can be concluded that at a 1.5% concentration, the PVA/Ag nanocomposite not only compensates for the solubility of PVA but also helps to stabilize and enhance the overall structure, creating a composite material with superior moisture resistance compared to the initial PLA. This hypothesis of structural improvement is fully compatible with the results of the surface morphology analysis (to be discussed in section 3.2), which shows that the film structure becomes denser at high silver nanoparticle concentrations.

Characterization of PLA/PVA-Ag Films

Morphological analysis by electron microscopy (SEM and TEM, Figure 2) provided profound visual evidence of the structural changes in the PLA film upon the integration of the PVA/Ag nanocomposite. SEM images revealed that the surface of the neat PLA control film (F/0.0) was completely smooth, dense, and homogeneous, which is the characteristic structure of a pure polymer film. In contrast, the surface of the PLA/PVA-Ag composite film exhibited a distinct, sponge-like, microporous structure. This structure is strong visual evidence that the hydrophilic PVA phase was leached out from the hydrophobic PLA matrix, leaving behind voids. This phenomenon is fully compatible with and serves as a visual explanation for the high water solubility results recorded previously.

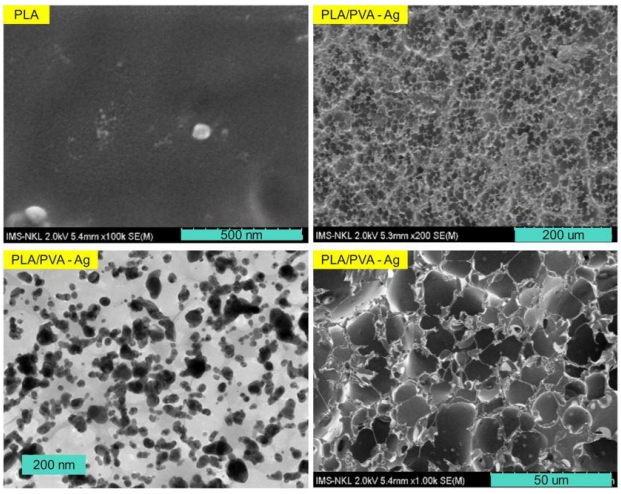

Figure 2: SEM image of PLA, and SEM and TEM images of PLA/PVA-Ag

At the nano-scale, transmission electron microscopy (TEM) analysis confirmed the presence and dispersion of silver nanoparticles within the material's structure. In the TEM image, the high-contrast dark spots, corresponding to regions of high electron density, were identified as the AgNPs. These nanoparticles have a size of less than 100 nm and are relatively uniformly dispersed in the light-colored polymer matrix. This result confirms that the synthesis method was successful in creating and incorporating the nanoparticles into the film, which is a prerequisite for the material to exhibit the desired antimicrobial and mechanical properties. In summary, the morphological analyses clarified that the material's structure is a porous polymer scaffold reinforced with dispersed silver nanoparticles.

FT-IR spectroscopy (Figure 3) was performed to confirm the chemical structure of the constituent materials and to verify their successful integration into the composite film. The spectrum of the neat PLA (poly(lactic acid)) film exhibits characteristic absorption peaks, including a strong and sharp peak at approximately 1750 cm^{-1} (C=O stretching vibration of the ester group) and a cluster of peaks in the 1080–1180 cm^{-1} region (C-O stretching vibration). Meanwhile, the spectrum of the PVA-Ag (poly(vinyl alcohol)-silver) nanocomposite is dominated by a broad and strong absorption band in the 3200–3500 cm^{-1} region, which is characteristic of the stretching vibration of hydrogen-bonded hydroxyl (-OH) groups [23-25].

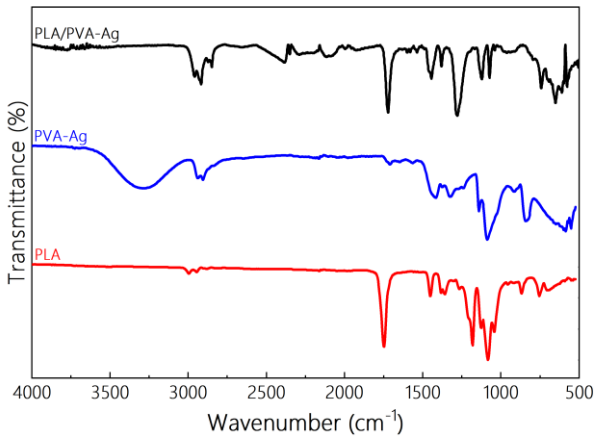

Figure 3: FT-IR spectra of PLA, PVA-Ag, and the PLA/PVA-Ag composite

The FT-IR spectrum of the final PLA/PVA-Ag composite film is a superposition of the constituent spectra, providing clear evidence of successful fabrication. Specifically, the simultaneous presence of the sharp C=O peak at ~1750 cm^{-1} (belonging to PLA) and the broad -OH band at ~3200–3500 cm^{-1} (belonging to PVA) in the same spectrum confirms that the PVA-Ag nanocomposite was dispersed within the PLA polymer matrix.

https://doi.org/10.62239/jca.2025.037

More importantly, the absence of any new significant absorption peaks or the disappearance of characteristic peaks indicates that no new covalent bonds were formed between the components. Therefore, it can be concluded that this combination is physical in nature, resulting from a blending process. The interactions between the two polymer phases are primarily secondary interactions, such as potential hydrogen bonding between the carbonyl (C=O) group of PLA and the hydroxyl (-OH) group of PVA. Thus, the FT-IR results have provided valid structural evidence, confirming the successful fabrication of the hybrid PLA/PVA-Ag composite film.

Antimicrobial Activity Evaluation

In addition to *E. coli* (a major foodborne pathogen) and *S. cerevisiae* (a key food spoilage agent), *B. subtilis* was tested as a representative spore-forming Gram-positive bacterium. Its endospores resist conventional sterilization, which kills vegetative cells. The successful inhibition of *B. subtilis* would confer substantial practical value upon it in the field of food preservation films. The experimental results demonstrate that the PLA/PVA/Ag composite film exhibits broad-spectrum antimicrobial activity, effectively inhibiting the growth of Gram-positive bacteria (*B. subtilis*), Gram-negative bacteria (*E. coli*), and yeast (*S. cerevisiae*). Data analysis indicates that the control sample and the neat PLA film showed no significant antimicrobial capability, with the number of surviving colonies being nearly equivalent. This confirms the bio-inert nature of PLA. In contrast, all PLA/PVA/Ag composite films markedly reduced the number of surviving microorganisms.

More importantly, the antimicrobial activity was clearly dose-dependent. As the content of the PVA-Ag colloid was increased from 0.5 mL to 1.0 mL and 1.5 mL, the number of colonies consistently decreased across all three microbial strains. The PLA/PVA-Ag 1.5 mL sample always showed the most potent inhibitory effect, with the lowest number of surviving microorganisms in all tests. This demonstrates that a higher concentration of the antimicrobial agent leads to a stronger microbicidal effect.

The antimicrobial mechanism of the material is attributed to the presence of silver nanoparticles (AgNPs) within the film's structure. These nanoparticles act as a reservoir for the slow release of silver ions (Ag^+) into the surrounding medium. Ag^+ ions are highly toxic to microorganisms through multiple simultaneous mechanisms: (1) interacting with sulfur-containing proteins in the cell membrane, thereby disrupting its structure and function; (2) inhibiting the activity of essential respiratory enzymes; and (3) causing DNA damage, which prevents replication. This multi-target and non-specific attack mechanism explains the material's broad-spectrum antimicrobial activity, making it effective against various types of microorganisms.

These results demonstrate that the integration of the PVA-Ag nanocomposite successfully imparted strong, dose-dependent, and broad-spectrum antimicrobial properties to the PLA film, opening up great potential for the material's application in the field of active food packaging.

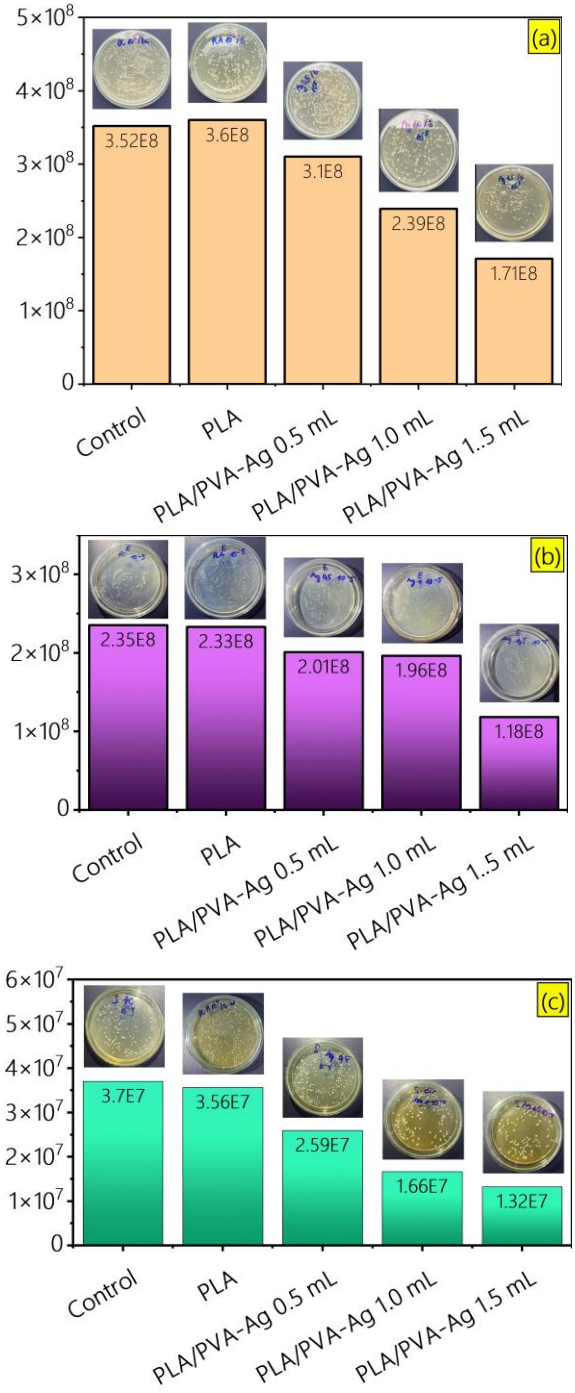

Figure 4: Antimicrobial test results against B. subtilis (a), E. coli (b), and S. cerevisiae (c)

Conclusion

This study successfully fabricated PLA/PVA/Ag nanocomposite films via the solvent casting and demonstrated the material's superior properties for food packaging applications. The incorporation of 1.0 wt% of the PVA/Ag nanocomposite significantly improved the tensile strength of the PLA film (~20%) while maintaining a homogeneous structure. More importantly, the composite material exhibited broad-spectrum antimicrobial activity, effectively inhibiting the growth of both Gram-positive and Gram-negative bacteria, and yeast, with an efficacy that increased with the concentration of nanoparticles. These findings confirm that the integration of PVA-Ag is an effective and viable strategy for developing PLA-based active packaging materials, contributing to ecologically sustainable parking solution that enhance food safety and shelf life.

References

1. R.-S. Yu, Y.-F. Yang, S. Singh, Front. Mar. Sci., 10 (2023) 1305091. https://doi.org/10.3389/fmars.2023.1305091
2. L.K. Ncube, A.U. Ude, E.N. Ogunmuyiwa, R. Zulkifli, I.N. Beas, Materials (Basel), 13 (2020) 4994. https://doi.org/10.3390/ma13214994
3. T.A. Swetha, A. Bora, K. Mohanrasu, P. Balaji, R. Raja, K. Ponnuchamy, G. Muthusamy, A. Arun, Int. J. Biol. Macromol., 234 (2023) 123715. https://doi.org/10.1016/j.ijbiomac.2023.123715
4. N. Mallegni, T.V. Phuong, M.-B. Coltelli, P. Cinelli, A. Lazzeri, Materials (Basel), 11 (2018) 148. https://doi.org/10.3390/ma11010148
5. E. Sritham, P. Phunsombat, J. Chaishome, MATEC Web Conf., 192 (2018) 03014. https://doi.org/10.1051/matecconf/201819203014
6. L. Shao, Y. Xi, Y. Weng, Molecules, 27 (2022) 5953. https://doi.org/10.3390/molecules27185953
7. P.R. Govindarajan, S. Chinnusamy, A.B. Kolekar, J.A. Antony, J. Appl. Polym. Sci., n/a (2023) e57541. https://doi.org/10.1002/app.57541
8. L. An, X. Hu, P. Perkins, T. Ren, Front. Nutr., 9 (2022) 924304. https://doi.org/10.3389/fnut.2022.924304
9. T.C. Dakal, A. Kumar, R.S. Majumdar, V. Yadav, Front. Microbiol., 7 (2016) 1831. https://doi.org/10.3389/fmicb.2016.01831
10. E.O. Mikhailova, Antibiotics (Basel), 14 (2024) 5. https://doi.org/10.3390/antibiotics14010005
11. K. Shameli, M.B. Ahmad, W.M. Yunus, N.A. Ibrahim, R.A. Rahman, M. Jokar, M. Darroudi, Int. J. Nanomed., 5 (2010) 573–579. https://doi.org/10.2147/ijn.s12007
12. N. Vidakis, M. Petousis, E. Velidakis, M. Liebscher, L. Tzounis, Biomimetics (Basel), 5 (2020) 42. https://doi.org/10.3390/biomimetics5030042
13. B. Zhu, C. Fan, C. Cheng, T. Lan, L. Li, Y. Qin, J. Food Sci., 86 (2021) 2481–2492. https://doi.org/10.1111/1750-3841.15746
14. Y. Qi, H.-L. Ma, Z.-H. Du, B. Yang, J. Wu, R. Wang, X.-Q. Zhang, ACS Omega, 4 (2019) 21439–21449. https://doi.org/10.1021/acsomega.9b03132
15. K. Pušnik Črešnar, A. Aulova, D.N. Bikiaris, D. Lambropoulou, K. Kuzmič, L. Fras Zemljič, Molecules, 26 (2021) 4161. https://doi.org/10.3390/molecules26144161.
16. P.K. Agrawal, P. Sharma, V. Singh, S. Chauhan, J. Mater. Environ. Sci., 14(5) (2023) 560–581.
17. S. Asano, Adv. Mater. Sci. Res., 7(5) (2024) 199–200. https://doi.org/10.37532/aaasmr.2024.7(5).199-200
18. Y. Liu, H. Wei, Z. Wang, Q. Li, N. Tian, Polym. (Basel), 10 (2018) 1178. https://doi.org/10.3390/polym10101178
19. A. Kyrychenko, D.A. Pasko, O.N. Kalugin, Phys. Chem. Chem. Phys., 19 (2017) 8742–8752. https://doi.org/10.1039/C6CP05562A
20. O. Velgosova, L. Mačák, E. Múdra, M. Vojtko, M. Lisnichuk, Polym. (Basel), 15 (2023) 379. https://doi.org/10.3390/polym15020379
21. Y. Zare, Compos. Part A Appl. Sci. Manuf., 84 (2016) 158–164. https://doi.org/10.1016/j.compositesa.2016.01.020.
22. J. Huang, J. Zhou, M. Liu, JACS Au, 2 (2022) 280–288. https://doi.org/10.1021/jacsau.1c00430
23. Z. Liu, H. Lu, H. Zhang, L. Li, J. Appl. Polym. Sci., 138 (2021) 51204. https://doi.org/10.1002/app.51204
24. Z. Yan, Q. Dou, J. Vinyl Addit. Technol., 30 (2024) 895–905. https://doi.org/10.1002/vnl.22093
25. B. Smith, Spectroscopy, 37 (2022) Article ID ly3071f5. https://doi.org/10.56530/spectroscopy.ly3071f5